Investigation on heat and mass transfer performance of novel composite strontium chloride for sorption reactors

L.Jiang[a,b,*], Y.J. Lu[b], K. Tang[b], Y.D. Wang[b], Ruzhu Wang[a], A.P. Roskilly[b], Liwei Wang[a]

[a] *Institute of Refrigeration and Cryogenics, Shanghai Jiao Tong University, Shanghai, 200240, China*

[b] *Sir Joseph Swan Centre for Energy Research, Newcastle University, Newcastle NE1 7RU, UK*

Abstract: A novel composite strontium chloride ($SrCl_2$) is developed with porous material of expanded natural graphite (ENG) and nanoparticle of carbon coated aluminum (Al@C) as the additives. Samples with different densities and mass ratios of salt are produced and classified into disk and plate types which are parallel and perpendicular to the compression direction, respectively. Thermal conductivity is investigated by the laser flash measuring method whereas permeability is tested through the Ergun model. It is indicated that with regard to thermal conductivity and permeability, plate samples show the better performance than that of disk samples. The highest thermal diffusivity could reach 5.7 $mm^2 \cdot s^{-1}$ when the density is 800 $kg \cdot m^{-3}$. Correspondingly the highest thermal conductivity is 2.96 $W \cdot m^{-1} \cdot K^{-1}$, which is about 15 times higher than that of ordinary granular $SrCl_2$. Permeability of plate and disk samples range from 9.9×10^{-10} m^2 to 9.89×10^{-14} m^2 and 2.91×10^{-10} m^2 to 2.46×10^{-14} m^2 when the density ranges between 400 $kg \cdot m^{-3}$ and 600 $kg \cdot m^{-3}$. The possible applications are presented and compared by using heat and mass properties of novel composite $SrCl_2$, which show their respective advantages when simulating the performance for the different reactors.

Keywords: Composite strontium chloride, Nanoparticle, Expanded natural graphite, Sorption reactor

** Corresponding author. Tel. +86-21-34206309*

Email: maomaojianglong@sjtu.edu.cn (L. Jiang)

Nomenclature

A	Area of sample cross section (m^2)
Al@C	Carbon coated aluminum
B	Shape factor
C	Specific heat ($J \cdot g^{-1} \cdot K^{-1}$)
d	Thickness of sample (mm)
ENG	Expanded natural graphite
ENG-TSA	Expanded natural graphite treated with sulfuric acid
K	Permeability (m^2)
m	Mass flow rate ($kg \cdot s^{-1}$)
MWCNT	Multi-walled carbon nanotube
p	Pressure (Pa)
q	Gas volume flow rate ($L \cdot min^{-1}$)
R	Gas constant ($J \cdot kg^{-1} \cdot K^{-1}$)
SCP	Specific cooling power ($W \cdot kg^{-1}$)
STES	Sorption thermal energy storage
T	Temperature (°C)
TES	Thermal energy storage
t	Time (s)

Greek letters

α	Thermal diffusivity ($mm^2 \cdot s^{-1}$)
λ	Thermal conductivity ($W \cdot m^{-1} \cdot K^{-1}$)
μ	Gas viscosity (Pa·s)
v	Axial velocity ($m \cdot s^{-1}$)

Subscripts

a	Axial
con	Condensation
de	Desorption

in	Inlet
out	Outlet
$SrCl_2$	Strontium chloride
sorb	Sorbent

1. Introduction

Sorption reaction process has drawn a burgeoning number of attentions due to its advantages of simple structure and utilizing green refrigerants without Ozone Depletion Potential (ODP) and Global Warming Potentials (GWP) [1, 2]. It is worth noting that sorption reaction process can be applied to both refrigeration and thermal energy storage (TES). For sorption refrigeration, specific cooling power (SCP) plays a leading role when considering the system compactness. As for sorption thermal energy storage (STES), heat releasing power is paramount with regard to the different demands of end users. Both SCP and heat releasing power are relevant with cycle time, which is mainly determined by the heat and mass transfer performance of the sorbent.

For heat and mass transfer enhancement, composite sorbent is considered as one effective method which has been widely investigated. As a major matrix of composite sorbent, expanded natural graphite (ENG) has been selected for physical and chemical sorbents[3], which was first invented by Carburet Company in US [4]. Mauran et al.[5] introduced ENG as a matrix to the consolidated composite sorbent, which demonstrated the better thermal conductivity for composite metal chlorides. Tian et al.[6] investigated the heat and mass transfer performance for $CaCl_2$ composite sorbents. Results revealed that the highest thermal conductivity was able to reach 1.66 $W \cdot m^{-1} \cdot K^{-1}$ in term of different densities and mass ratios of salt. Tamainot-Telto and Critoph [7, 8] tested the thermal conductivity of activated carbon by using the steady-state heat source method, and evaluated the performance for heat pump application. Later, Jiang et al [9, 10] investigated thermal conductivity and permeability of eight different chlorides with ENG, and compared the properties of different consolidated

composite sorbents in the sorption process. Besides, expanded natural graphite treated by sulfuric acid (ENG-TSA) was recently introduced to further improve the thermal conductivity of metal chlorides [11, 12]. The highest thermal conductivity of the composite sorbent was able to reach 88.1 $W \cdot m^{-1} \cdot K^{-1}$ while the permeability decreased to the magnitude of 10^{-14} m^2[13]. Nonetheless, one drawback is that price of ENG-TSA was about 60 times higher than that of ENG, and the limited improvement could be achieved for the real sorption refrigeration system[14, 15]. It is worth noting that thermal conductivity of the composite sorbent has improved significantly through various matrix when compared with that of granular chlorides. Comparably, mass transfer performance is stagnated or even slightly backwards.

Except for selecting ENG as the matrix, quite a lot of researchers have also focused on improving heat and mass transfer performance by using carbon nanomaterials in recent years. Due to the excellent heat transfer performance, nanoparticles such as multi-walled carbon nanotubes(MWCNT), graphite nanoplatelets, and carbon coated copper were attempted to be selected as the additives for the development of compound organic materials[16-18]. However, less research of composite sorbents is reported to improve heat and mass transfer performance by using carbon nanomaterials as the additives. The sorption performance of ammonia on the packed multi-walled carbon nanotubes was studied by Yan et al. Results indicated that pure MWCNT could be selected as additive for chemical sorbents to improve their heat transfer characteristics though it was not suitable for solid–gas sorption refrigeration owing to its relatively low sorption quantity[19]. Later, Yan et al.[20] investigated sorption characteristics of composite $CaCl_2$ with MWCNT as the matrix, and found that adding MWCNT into chemical sorbents could avoid the agglomeration phenomenon and prevent the sorption performance attenuation of the pure salt. Since carbon nanotubes are usually aggregated and entangled together, it is not easy to be dispersed homogeneously. Compared with carbon nanotubes, nanoparticles such as carbon coated metal with core-shell structure indicate large potentials for developing the composite sorbents. It reveals

that carbon coating is able to protect the external condition for the metal core, and the metal core can take a promoting effect while maintaining the excellent thermo-physical properties[21, 22]. The granular shape in nanometer size tends to be easy to occupy the porous structure of composite sorbents with ENG. As a result, it could avoid great swelling and agglomeration in the mass transfer process.

In this paper, strontium chloride ($SrCl_2$) impregnated with both ENG and carbon coated Aluminum (Al@C) as the additives is investigated for the comprehensive heat and mass performance since there is little research work about the composite $SrCl_2$ with these two additives. Due to the anisotropic thermal conductivity and permeability of compact ENG[23], novel composite $SrCl_2$ is investigated and compared in term of disk and plate samples, which are parallel and perpendicular to the compression direction respectively.

2. Development of novel composite $SrCl_2$

Compared with the conventional composite sorbent, the novelty is to introduce the nanoparticle and porous material i.e. Al@C and ENG into the sorbent for the improvement of heat and mass transfer performance. Al@C is expected to further improve the mass transfer of the sorbent whereas ENG is conducive to the heat transfer performance. The thermochemical reaction process of $SrCl_2$ with ammonia can be according to the equations 1-2.

The development processes of the novel composite $SrCl_2$ can be referred to the reference[24]. ENG is expanded by the optimal expanding process, i.e. heating untreated natural graphite in an oven at the temperature of 600^{o}C for 8 minutes[25]. First, ENG is dried in the oven with controlled temperature of 120^{o}C. Meanwhile, the nanoparticle i.e. Al@C is dispersed in ethanol with ultrasonic bath for 30 minutes to prevent the aggregation of Al@C in the mixing process. $SrCl_2$, ENG and Al@C are stirred and mixed together by the ultrasonic treatment for another 30 minutes. The mixture will be dried in an oven at 120^{o}C for 48 h. Finally, the mixture is put into a vessel and pressed by the compression machine.

In the development of the novel composite $SrCl_2$, mass ratio of salt and density are two major factors. The crack will easily happen if the density is lower than 400 $kg \cdot m^{-3}$, which results in the poor mechanical stability of the composite sorbent. Also worth noting that the higher density and lower mass ratio of salt are, the lower permeability and the higher thermal conductivity will become. For testing the thermal properties, density of the novel composite $SrCl_2$ is selected in the range from 500 $kg \cdot m^{-3}$ to 800 $kg \cdot m^{-3}$ for good mechanical stability. The mass ratio between $SrCl_2$ and ENG ranges from 50% to 83% i.e. from 1:1 to 5:1 whereas the ratio between ENG and Al@C is adopted as 20:1[24]. Since anisotropic characteristics of the consolidated ENG matrix have been studied[23], both plate and disk samples are developed for comparison which are indicated in Fig.1. For disk samples shown in Fig.1a, heat and mass transfer testing direction is parallel to the compression direction. For plate samples shown in Fig.1b, the testing direction is perpendicular to the compression direction.

$$SrCl_2 \cdot NH_3 + 7NH_3 \longleftrightarrow SrCl_2 \cdot 8NH_3 + 7\Delta H_{SrCl_2} \quad (1)$$

$$NH_3(gas) \longleftrightarrow NH_3(liq) + \Delta H_{con} \quad (2)$$

In order to observe the elements distribution, the novel composite $SrCl_2$ is investigated by a Scanning Electron Microscopy (SEM) and Energy Dispersive X-ray spectroscopy (DEX) which are shown in Fig.2. Fig.2a indicates the SEM image of the sample, which illustrates the surface morphology. Fig.2b and Fig.2c show the distribution of element Al and Cl, which illustrates the uniformity of nanoparticles and salts.

3. Testing method of the novel composite $SrCl_2$

3.1. Thermal conductivity

Thermal conductivity is investigated by the Laser flash method. Fig.3 demonstrates the diagram of the testing equipment, i.e. LFA467 instrument. The testing unit is mainly composed of heater, optical filter, infrared detector, sample changer, reflector and flash lamp. As testing temperature T is controlled by a furnace heated condition, a beam of light pulse is emitted by the laser instantaneously, which is uniformly illuminating in the sample surface. The temperature transient increases from the hot end of one-dimensional heat conduction to the

cold end propagation. The temperature could be monitored by means of an infrared detector, which is calibrated by liquid nitrogen. The thermal diffusivity could be determined through the curve of temperature vs. time.

Since the width of the optical pulse is infinitely small, heat conduction of the testing sample is regarded as one-dimensional heat transfer. The semi-heating time t_{50} is evaluated by the equation 3:

$$\alpha = \frac{0.1388 \cdot d^2}{t_{50}} \tag{3}$$

where α is the thermal diffusivity ($mm^2 \cdot s^{-1}$), d is the thickness of testing samples (mm), t_{50} is the semi-heating time (s).

$$\lambda(T) = \alpha(T) \cdot C_p(T) \cdot \rho(T) \tag{4}$$

where $\lambda(T)$ is the thermal conductivity at a testing temperature ($W \cdot m^{-1} \cdot K^{-1}$), $\alpha(T)$ is the thermal diffusivity ($mm^2 \cdot s^{-1}$), C_p is the specific heat ($J \cdot g^{-1} \cdot K^{-1}$), $\rho(T)$ is the density of the sample ($kg \cdot m^{-3}$). The random error of the testing equipment is less than 0.1%, and the largest relative error is 5%.

3.2. Permeability

Fig.4a shows the schematic diagram of the permeability testing system whereas Fig.4b indicates the photo of the system. In the experiment the sorbent will be placed in the chamber of the test unit to simulate the real sorption system. The testing unit is mainly composed of the sample chamber, pressure difference transmitter and the rotermeter. When the gas nitrogen is flowing through the sample with flow rate q_v, pressure drop Δp will be measured. To obtain the permeability K, parameters Y and X are evaluated through the testing data of flow rate, the outlet gas pressure and pressure drop, etc. 1/K is the intercept of the linear fitting line of Y and X.

Since the testing samples are porous media with very low velocities, Darcyan and non-Darcyan permeability parameters should be both considered. Therefore, Ergun model is applicable in the measurement and no compressibility effects exist[26]. Intrinsic characteristic of the material can be according to the equations 5 and 6:

$$Y = BX + \frac{1}{K} \tag{5}$$

in which

$$Y = \frac{(P_{in}^{\ 2} - P_{out}^{\ 2})S}{2RT\mu m_a \Delta z}; \qquad X = \frac{m_a}{\mu S}; \qquad m_a = \rho A v_a \tag{6}$$

where K is the permeability of the samples (m^2), B is the shape factor, P_{in} and P_{out} are the inlet and outlet pressure of the gas nitrogen, A is the area of sample cross section (m^2), R is the gas constant ($J \cdot kg^{-1} \cdot K^{-1}$), T is the sample temperature (K) which doesn't change greatly, Δz is the thickness of the sample, μ and ρ are the gas viscosity (Pa·s) and density ($kg \cdot m^{-3}$), respectively; m_a is the mass flow rate of the gas ($kg \cdot s^{-1}$), v_a is the axial velocity ($m \cdot s^{-1}$).

The error of permeability can be expressed as equation 7:

$$\left|\frac{dK}{K}\right| = \left|\frac{dY - BdX}{Y - BX}\right| \le \left|\frac{dY}{Y - BX}\right| + \left|\frac{BdX}{Y - BX}\right| \tag{7}$$

The pressure is investigated by the environmental temperature. The differential pressure that is tested by the differential pressure meter with the error of 0.5%, and the gas mass flowrate is tested by the flow meter with the error of 4%. The average relative error of K is calculated, and the error of permeability is 5.08%.

4. Experimental results and discussions

4.1. Thermal diffusivity

Since the samples with different densities and mass ratios of salt show the similar trends, mass ratios of 50% between $SrCl_2$ and ENG as well as densities from 500 $kg \cdot m^{-3}$ to 800 $kg \cdot m^{-3}$ are selected for further elaboration of thermal diffusivity, which are shown in Fig.5. Fig.5a and Fig.5b indicate the thermal diffusivity of both disk and plate samples under the condition of different testing temperatures from 20°C to 100°C. It is demonstrated that the thermal diffusivity increases with the decrease of testing temperature. This is mainly because the higher temperature usually results in the friable structure of the novel composite $SrCl_2$, which leads to the larger thermal contact resistance inside. Also worth noting that thermal diffusivity of plate samples are much higher than that of disk samples due to the anisotropic characteristic of ENG. The highest thermal diffusivity of disk and plate samples are able to reach 1.94 $mm^2 \cdot s^{-1}$ and 5.7 $mm^2 \cdot s^{-1}$, respectively when the testing temperature is 20°C. For

different testing temperatures, thermal diffusivities of the plate and disk samples are in the range from 1.72 $mm^2 \cdot s^{-1}$ to 1.94 $mm^2 \cdot s^{-1}$ and 4.47 $mm^2 \cdot s^{-1}$ to 5.7 $mm^2 \cdot s^{-1}$, respectively.

Also for evaluating the thermal stability of the novel composite $SrCl_2$, thermal diffusivity of disk samples with the density of 800 $kg \cdot m^{-3}$ is presented and compared among different shot times which is shown in Fig.6. It could be found that the testing difference among the different shot times becomes close when the testing temperature increases from 20°C to 100°C. Since the equilibrium reaction temperature of the $SrCl_2$ is about 95°C in term of 30°C heat sink temperature, it reveals the good repeatability of thermal diffusivity in its working range.

In order to comprehensively analyze the thermal diffusivity, samples with different densities and mass ratios of salt are evaluated and compared when the temperature is selected as 20°C. Fig.7 indicates the thermal diffusivity of the novel composite $SrCl_2$ with densities and mass ratios ranging from 500 $kg \cdot m^{-3}$ to 800 $kg \cdot m^{-3}$ and from 50% to 83%, respectively. It is demonstrated that thermal diffusivity of both disk and plate samples increases with the decrease of mass ratio. For disk samples, thermal diffusivity decreases slightly with the increase of the density. Comparably, thermal diffusivity of plate samples increases with the increase of the density. For different densities and mass ratios of salt, thermal diffusivity of disk and plate samples ranges from 1.54 $mm^2 \cdot s^{-1}$ to 1.94 $mm^2 \cdot s^{-1}$ and 2.09 $mm^2 \cdot s^{-1}$ to 5.7 $mm^2 \cdot s^{-1}$.

4.2. Thermal conductivity

According to the Laser flash measuring method, thermal conductivity of the novel composite $SrCl_2$ can be calculated by the equation 4, in which the specific heat can be evaluated by the equation 8. Since the ratio of the Al@C accounts for quite a small part of the total novel composite sorbent, $SrCl_2$ and ENG will have the major influence on the specific heat of the novel composite sorbent. Therefore, ENG will be more conducive than Al@C with respect to thermal conductivity. Comparably, Al@C is expected for the improvement of permeability.

Similar as the thermal diffusivity with 20°C testing temperature, thermal conductivity of disk and plate samples is investigated and compared when the densities and mass ratios of salt are selected from 500 $kg \cdot m^{-3}$ to 800 $kg \cdot m^{-3}$ and from 50% to 83%, respectively, which is shown in Fig.8. Results demonstrate that the thermal conductivity of both disk and plate samples increase with the decrease of mass ratio of salt and the increase of the density. The highest thermal diffusivity of the novel composite $SrCl_2$ could reach 0.98 $W \cdot m^{-1} \cdot K^{-1}$ and 2.96 $W \cdot m^{-1} \cdot K^{-1}$ in term of disk and plate samples when the density and mass ratio are 800 $kg \cdot m^{-3}$ and 50%. The highest thermal conductivity of plate sample is about 15 times higher than that of ordinary granular $SrCl_2$. For different densities and mass ratios of salt, thermal conductivity of the disk and plate samples range from 0.44 $W \cdot m^{-1} \cdot K^{-1}$ to 0.98 $W \cdot m^{-1} \cdot K^{-1}$ and 0.58 $W \cdot m^{-1} \cdot K^{-1}$ to 2.96 $W \cdot m^{-1} \cdot K^{-1}$, respectively.

$$C_p = \beta \cdot C_{p,salt} + \gamma \cdot C_{p,ENG} + (1-\beta-\gamma) \cdot C_{p,Al@C} \quad (8)$$

where β is the mass ratio of $SrCl_2$ with respect to the total mass of the novel composite sorbent, γ is the mass ratio of ENG with respect to the total mass.

4.3. Permeability

Table 1 shows the permeability of the novel composite $SrCl_2$ with different densities from 400 kg/m^3 to 600 kg/m^3 and mass ratios of salt from 50% to 83%. It is worth noting that plate samples enjoy the better permeability than that of the disk samples. Results also indicate that for disk and plate samples permeability ranges from 2.91×10^{-10} m^2 to 2.46×10^{-14} m^2 and 9.9×10^{-10} m^2 to 9.89×10^{-14} m^2, respectively. Permeability increases with the decrease of the density and the increase of mass ratio. In order to have a general understanding of the novel composite $SrCl_2$, permeability of plate samples with Al@C is compared with that without Al@C which is shown in Fig.9. It is indicated that when permeability is relatively low, permeability increases slightly with the increase of the mass ratio. For the sorbent with mass ratio larger than 67%, permeability of composite $SrCl_2$ increases significantly. Also worth noting that for different densities and mass ratios of salt, samples with Al@C enjoy the higher permeability than that without Al@C. The permeability difference between the different

composite sorbents decreases with the increase of the density. Although ENG plays a leading role in the higher density due to its ratio, one remarkable fact is that the nanoparticle is conducive to the improvement of the mass transfer performance of the composite $SrCl_2$. The nanoparticle tends to be easier to occupy the porous structure of the composite $SrCl_2$ than that of pure salts, which avoids the serious swelling and agglomeration. If the ratio of Al@C is increased excessively, thermal conductivity will be affected. The mass transfer should be further improved in the premise that the heat transfer performance is desirable.

4.4. Different applications of the disk and plate sample

For the sorption reactors, it is acknowledged that the heat transfer direction is usually parallel to the compressing direction of the sorbents, which indicates that the same situation as the disk samples. Comparably, heat transfer direction of another sorption reactor is perpendicular to the compressing direction, i.e. the situation as the plate samples with relatively better heat and transfer performance. Better heat and mass transfer performance of the sorbent will result in the higher sorption and desorption rate, which leads to the higher SCP and system compactness if the heat transfer of fluid side is considered as the same. Nonetheless, it is the case for the sorption refrigeration. Considering for the STES, there may exist different scenarios, which depends on the various demands of the end users such as the mass limitation of the system and heat releasing power.

Fig.10a indicates the schematic of sorption reactor 1 in which heat transfer direction is perpendicular to the compressing direction of the composite sorbent whereas Fig.11a demonstrates the schematic of sorption reactor 2 in which the heat transfer direction is parallel to the compressing direction. Both reactor 1 and 2 act as the sorption unit, and it will be connected for the scaling applications with regard to different cold and heat demands as shown in photos of Fig.10b and Fig.11b[15, 27]. It is worth noting that anisotropic heat and mass transfer performance of the novel composite sorbent could have the respective advantages for sorption refrigeration and

STES by using the different kinds of sorption reactors. By changing the concentration swing of the ENG and Al@C, the heat and mass transfer performance can be adjusted to satisfy the different demands, which will be more flexible for real applications. Therefore, thermal conductivity and permeability of disk and plate composite $SrCl_2$ are key parameters when simulating the performance for different types of reactors.

In order to further demonstrate the method to evaluate the sorption reactors by using heat and mass transfer properties of the novel sorbent, sorption reactor 2 is exemplified and analyzed for TES application since it is common to be used in the real sorption systems. Table 2 demonstrates the main parameters for the sorption reactor 2 in the simulation. The mathematic models could be referred to our previous work[28], which are according to the coordinates of Fig.11a. Properties of the disk samples for the simulation are selected as the density of 500 $kg \cdot m^{-3}$ and mass ratio of salt from 50% to 80%, and property of the pure $SrCl_2$ is also used for comparison. Fig.12 indicates the power density of sorption reactor 2 by using the novel composite $SrCl_2$ with different mass ratios, which is classified into heat and cold power density. Power density is defined as the heat and cold power output with respect to the unit mass of the sorbent, which is the key parameter to assess the performance of STES. Results indicate that the highest cold and heat power density could reach 84 $W \cdot kg^{-1}$ and 126 $W \cdot kg^{-1}$, which is improved by 140% and 180% when compared with that of the pure $SrCl_2$. Even the lowest cold and heat power density could still be improved by 112% and 147% due to the heat and mass transfer enhancement. In fact, performance of the reactor 2 in the freezing condition will be further improved due to the better mass transfer performance. Both ENG and Al@C are indispensable for the improvement of novel composite $SrCl_2$. As for the sorption reactor 1, the similar results could also be obtained by using the different heat and mass transfer properties of plate samples.

The overall system compactness and cost saving are also analyzed as shown in Fig.13. For a sorption system with 2kW required cooling power, the required mass of novel composite $SrCl_2$ increases with the

increment of the mass ratio from 50% to 83% based on the simulation results, which ranges from 23.7 kg to 27 kg. Compared with the required mass of 57 kg pure $SrCl_2$, it is decreased up to 58%. Correspondingly, the volume of the sorption reactor could be reduced up to 27%. As the metal part of the reactor decreases with the decrease of the mass of the composite sorbent, both reductions of metal and composite sorbent will be considered for the overall cost saving. As Fig.13 shows, the overall cost of the sorption reactor could be reduced up to 23.3% by using the novel composite $SrCl_2$.

5. Conclusions

The novel composite $SrCl_2$ is developed with ENG and Al@C as the additive to improve the heat and mass transfer performance. The anisotropic characteristics of the samples are investigated and compared with that without adding the nanoparticles. Conclusions are yielded as follows:

[1] It is demonstrated that thermal diffusivity increases with the decrease of testing temperature. Thermal diffusivity of plate samples are much higher than that of disk samples. The highest thermal diffusivity of disk and plate samples are able to reach 1.94 $mm^2 \cdot s^{-1}$ and 5.7 $mm^2 \cdot s^{-1}$, respectively when the testing temperature is 20°C. For different testing temperatures, thermal diffusivities of the plate and disk samples are in the range from 1.72 $mm^2 \cdot s^{-1}$ to 1.94 $mm^2 \cdot s^{-1}$ and 4.47 $mm^2 \cdot s^{-1}$ to 5.7 $mm^2 \cdot s^{-1}$.

[2] It is demonstrated that thermal diffusivity of both disk and plate samples shows the similar trend with the increase of mass ratio but different trend with the increment of density. For different densities and mass ratios of salt, the thermal diffusivity of disk and plate samples ranges from 1.54 $mm^2 \cdot s^{-1}$ to 1.94 $mm^2 \cdot s^{-1}$ and 2.09 $mm^2 \cdot s^{-1}$ to 5.7 $mm^2 \cdot s^{-1}$. Thermal conductivity of disk and plate samples increases with the decrease of mass ratio of salt and the increase of the density. For different densities and mass ratios of salt, thermal conductivity of disk and plate samples ranges from 0.44 $W \cdot m^{-1} \cdot K^{-1}$ to 0.98 $W \cdot m^{-1} \cdot K^{-1}$ and 0.58 $W \cdot m^{-1} \cdot K^{-1}$ to 2.96 $W \cdot m^{-1} \cdot K^{-1}$.

[3] Plate samples enjoy the higher permeability than that of disk samples. For different disk and plate samples permeability ranges from 2.91×10^{-10} m^2 to 2.46×10^{-14} m^2 and 9.9×10^{-10} m^2 to 9.89×10^{-14} m^2, respectively. Permeability increases when the density decreases and mass ratio of salt increases. For different densities and mass ratios of salt, samples with Al@C enjoy the higher permeability than that without Al@C. The nanoparticle is conducive to the improvement of the mass transfer performance of the composite $SrCl_2$.

[4] Thermal conductivity and permeability of disk and plate composite $SrCl_2$ are important parameters when simulating the performance for the different types of reactors. By changing the concentration swing of the ENG and Al@C, the heat and mass transfer performance can be adjusted to satisfy the different demands, which will be more flexible for applications. For a sorption system with 2kW required cooling power, the overall cost of the sorption reactor could be reduced up to 23.3% by using the novel composite $SrCl_2$.

With the potentially wide use of energy conversion technologies for the low grade heat in the near future, sorption refrigeration and thermal energy storage technology with composite sorbent could be considered as a method to solve the problem for energy utilization. The composite sorbent with both ENG and carbon coated metal may be one effective method to further improve the system performance.

Acknowledgements

This research was supported by the National Natural Science Foundation of China under contract number (51606118), Innovative Research Groups under contract number (51521004) and Heat-STRESS project (EP/N02155X/1) funded by the Engineering and Physical Science Research Council of the UK.

References

[1] R.Z. Wang, X. Yu, T.S. Ge, T.X. Li, The present and future of residential refrigeration, power generation and

297 energy storage, Applied Thermal Engineering, 53 (2013) 256-270.

298 [2] A.P. Roskilly, P.C. Taylor, J. Yan, Energy storage systems for a low carbon future – in need of an integrated

299 approach, Applied Energy, 137 (2015) 463-466.

300 [3] X. Py, E. Daguerre, D. Menard, Composites of expanded natural graphite and in situ prepared activated

301 carbons, Carbon, 40 (2002) 1255-1265.

302 [4] J.H. Li, L.L. Feng, Z.X. Jia, Preparation of expanded graphite with 160 μm mesh of fine flake graphite,

303 Materials Letters, 60 (2006) 746-749.

304 [5] S. Mauran, P. Prades, F. L'Haridon, Heat and mass transfer in consolidated reacting beds for thermochemical

305 systems, Heat Recovery Systems and CHP, 13 (1993) 315-319.

306 [6] B. Tian, Z.Q. Jin, L.W. Wang, R.Z. Wang, Permeability and thermal conductivity of compact chemical and

307 physical adsorbents with expanded natural graphite as host matrix, International Journal of Heat and Mass

308 Transfer, 55 (2012) 4453-4459.

309 [7] Z. Tamainot-Telto, R.E. Critoph, Monolithic carbon for sorption refrigeration and heat pump applications,

310 Applied Thermal Engineering, 21 (2001) 37-52.

311 [8] Z. Tamainot-Telto, R.E. Critoph, Advanced solid sorption air conditioning modules using monolithic carbon–

312 ammonia pair, Applied Thermal Engineering, 23 (2003) 659-674.

313 [9] L. Jiang, L.W. Wang, Z.Q. Jin, B. Tian, R.Z. Wang, Permeability and Thermal Conductivity of Compact

314 Adsorbent of Salts for Sorption Refrigeration, Journal of heat transfer ASME, 134 (2012) 104503-104506.

315 [10] L. Jiang, L.W. Wang, Z.Q. Jin, R.Z. Wang, Y.J. Dai, Effective thermal conductivity and permeability of

316 compact compound ammoniated salts in the adsorption/desorption process, International Journal of Thermal

317 Sciences, 71 (2013) 103-110.

318 [11] L.W. Wang, S.J. Metcalf, R.E. Critoph, R. Thorpe, Z. Tamainot-Telto, Thermal conductivity and

permeability of consolidated expanded natural graphite treated with sulphuric acid, Carbon, 49 (2011) 4812-4819.

[12] L.W. Wang, S.J. Metcalf, R.E. Critoph, R. Thorpe, Z. Tamainot-Telto, Development of thermal conductive consolidated activated carbon for adsorption refrigeration, Carbon, 50 (2012) 977-986.

[13] L. Jiang, L.W. Wang, R.Z. Wang, Investigation on thermal conductive consolidated composite $CaCl_2$ for adsorption refrigeration, International Journal of Thermal Sciences, 81 (2014) 68-75.

[14] Q.W. Pan, R.Z. Wang, L.W. Wang, D. Liu, Design and experimental study of a silica gel-water adsorption chiller with modular adsorbers, International Journal of Refrigeration, 67 (2016) 336-344.

[15] L. Jiang, L.W. Wang, C.Z. Liu, R.Z. Wang, Experimental study on a resorption system for power and refrigeration cogeneration, Energy, 97 (2016) 182-190.

[16] C. Selvam, D.M. Lal, S. Harish, Thermal conductivity enhancement of ethylene glycol and water with graphene nanoplatelets, Thermochimica Acta, 642 (2016) 32-38.

[17] R.L. Poveda, G. Dorogokupets, N. Gupta, Carbon nanofiber reinforced syntactic foams: Degradation mechanism for long term moisture exposure and residual compressive properties, Polymer Degradation and Stability, 98 (2013) 2041-2053.

[18] P. Kumar, S. Yu, F. Shahzad, S.M. Hong, Y.-H. Kim, C.M. Koo, Ultrahigh electrically and thermally conductive self-aligned graphene/polymer composites using large-area reduced graphene oxides, Carbon, 101 (2016) 120-128.

[19] T. Yan, T.X. Li, R.Z. Wang, R. Jia, Experimental investigation on the ammonia adsorption and heat transfer characteristics of the packed multi-walled carbon nanotubes, Applied Thermal Engineering, 77 (2015) 20-29.

[20] T. Yan, T.X. Li, H. Li, R.Z. Wang, Experimental study of the ammonia adsorption characteristics on the composite sorbent of $CaCl_2$ and multi-walled carbon nanotubes, International Journal of Refrigeration, 46 (2014)

165-172.

[21] C. Lei, S. He, Z. Du, F. Pan, Q. Zhu, H. Li, Effects of gas composition and temperature on the fluidization characteristics of carbon-coated iron ore, Powder Technology, 301 (2016) 608-614.

[22] C. Vales-Pinzon, R.A. Medina-Esquivel, J. Ordonez-Miranda, J.J. Alvarado-Gil, Thermal transfer in mixtures of ethylene glicol with carbon coated iron nanoparticles under the influence of a uniform magnetic field, Journal of Alloys and Compounds, 643, Supplement 1 (2015) S71-S74.

[23] L.W. Wang, Z. Tamainot-Telto, S.J. Metcalf, R.E. Critoph, R.Z. Wang, Anisotropic thermal conductivity and permeability of compacted expanded natural graphite, Applied Thermal Engineering, 30 (2010) 1805-1811.

[24] Q. Wu, X. Yu, H. Zhang, Y. Chen, L. Liu, X. Xie, K. Tang, Y. Lu, Y. Wang, A.P. Roskilly, Fabrication and thermal conductivity improvement of novel composite adsorbents adding with nanoparticles, Chinese journal of mechanical engineering, 6 (2016) 1114-1118.

[25] Z. Jin, B. Tian, L. Wang, R. Wang, Comparison on Thermal Conductivity and Permeability of Granular and Consolidated Activated Carbon for Refrigeration, Chinese Journal of Chemical Engineering, 21 (2013) 676-682.

[26] L.W. Wang, S.J. Metcalf, R.E. Critoph, Z. Tamainot-Telto, R. Thorpe, Two types of natural graphite host matrix for composite activated carbon adsorbents, Applied Thermal Engineering, 50 (2013) 1652-1657.

[27] L. Jiang, R.Z. Wang, L.W. Wang, P. Gao, F.Q. Zhu, Investigation on gradient thermal cycle for power and refrigeration cogeneration, International Journal of Refrigeration, 76 (2017) 42-51.

[28] L. Jiang, L. Wang, A.P. Roskilly, R. Wang, Design and performance analysis of a resorption cogeneration system, International Journal of Low-Carbon Technologies, 8 (2013) 85-91.

364

365

366 **List of Figures**

385

386
387

388

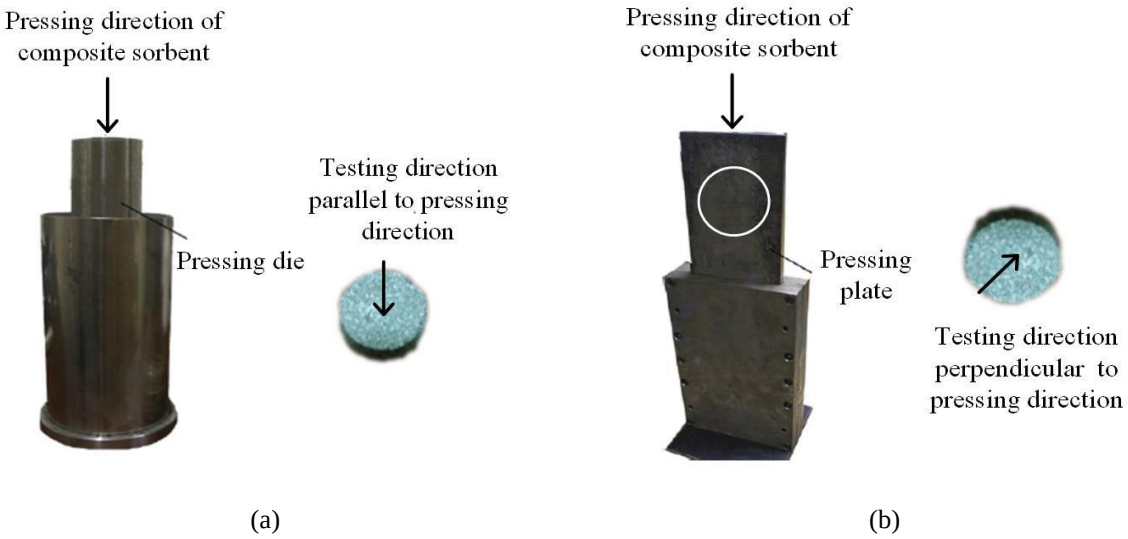

Fig.1. The compressing rig and novel composite $SrCl_2$ (a) disk samples; (b) plate samples.

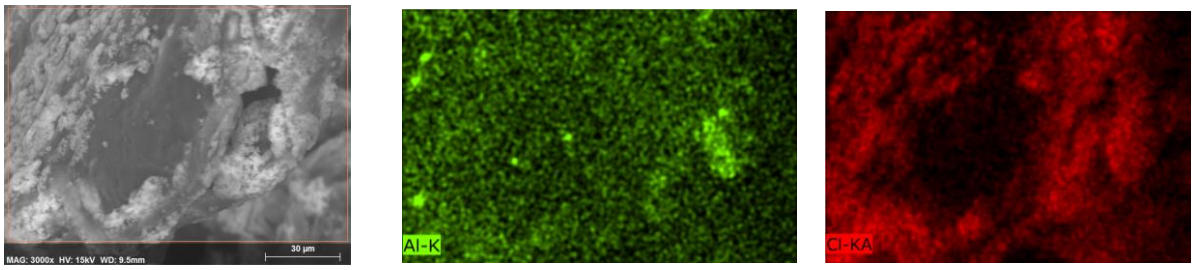

(a) (b) (c)

Fig.2. SEM image and EDX mapping of the novel composite $SrCl_2$ (a) SEM; (b) EDX Mapping of the element Al; (c) EDX Mapping of the element Cl.

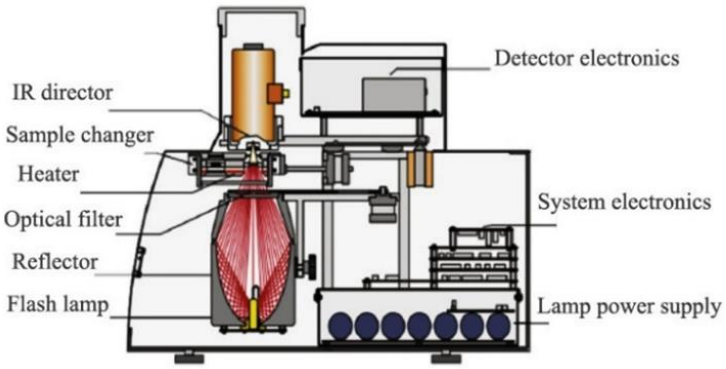

Fig.3. Schematic of thermal conductivity testing unit.

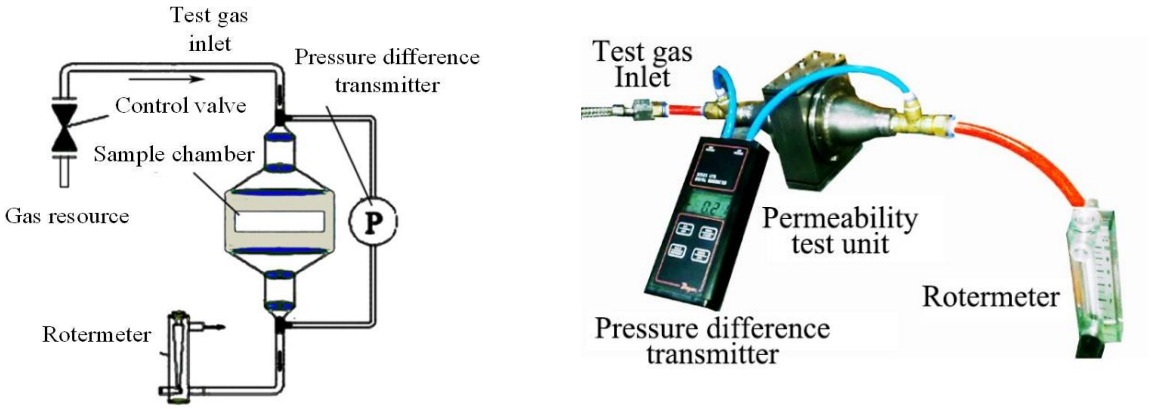

(a) (b)

435 Fig.4. The permeability test system (a) schematic; (b) photo.

436

437

438

439

440

441

442

443

444

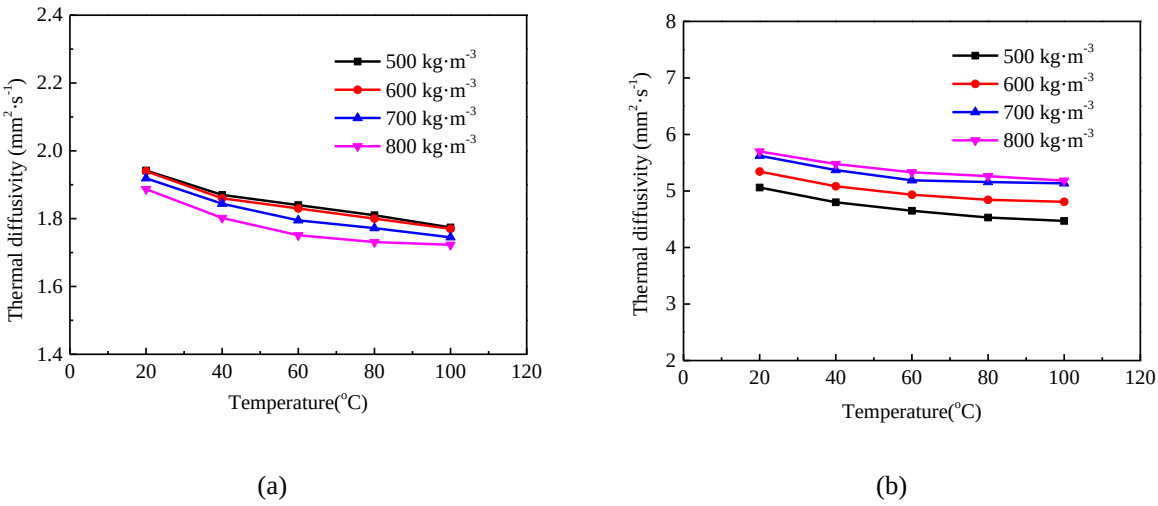

445 Fig.5. Thermal diffusivity of the novel composite $SrCl_2$ vs. different testing temperatures (a) disk samples;

446 (b) plate samples.

447

448

449

450

451

452

453

454

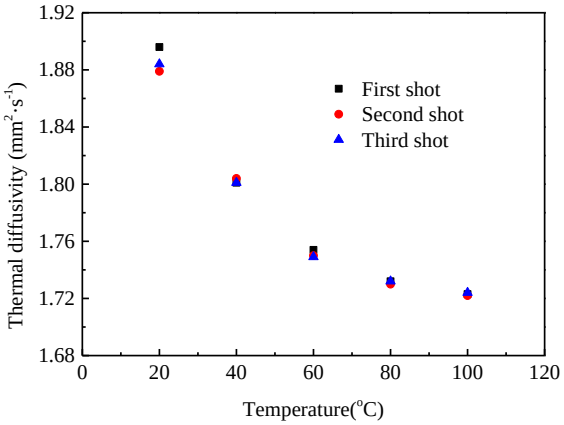

Fig.6. Thermal diffusivity of disk samples of the novel composite $SrCl_2$ vs. different shot times.

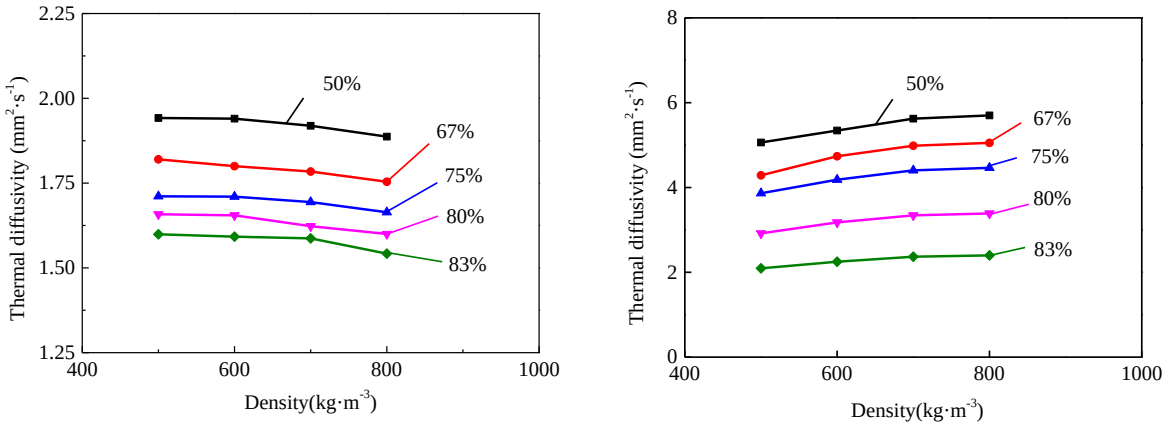

(a) (b)

Fig.7. Thermal diffusivity of the novel composite $SrCl_2$ vs. different densities and mass ratios of salt (a) disk samples; (b) plate samples.

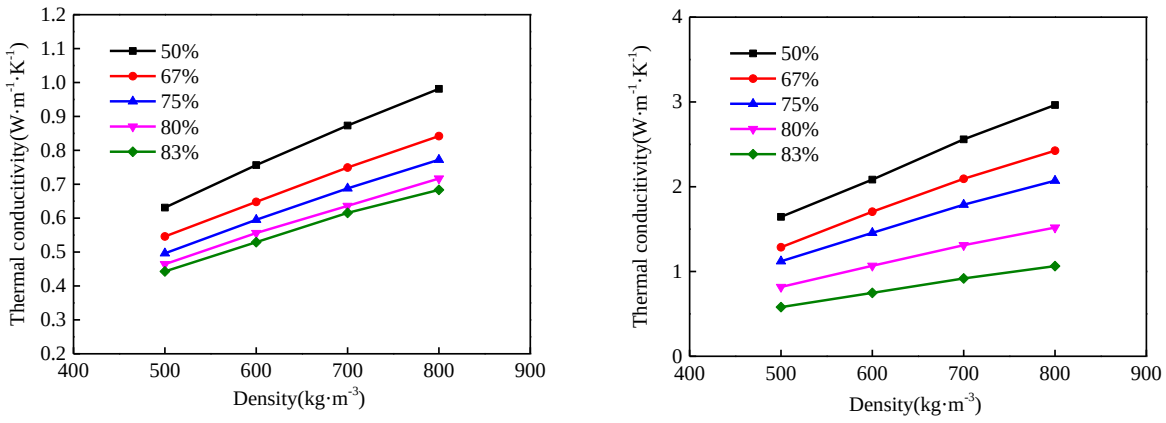

479 Fig.8. Thermal conductivity of the novel composite $SrCl_2$ vs. different densities and mass ratios (a) disk samples;

480 (b) plate samples.

481

482

483

484

485

486

487

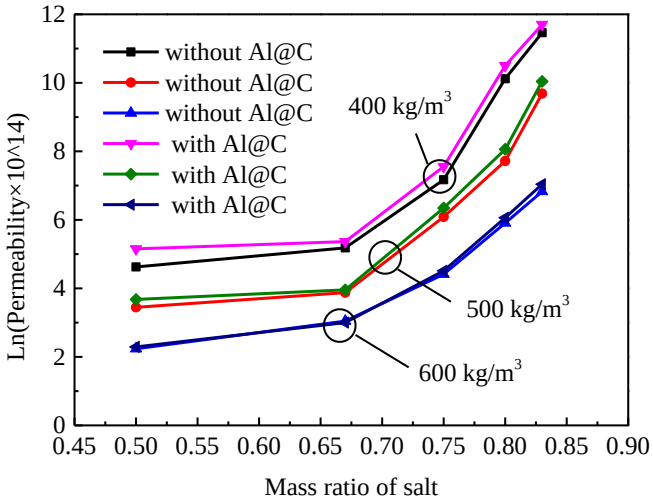

Fig.9. Permeability of plate samples of composite $SrCl_2$ with and without Al@C vs. different mass ratios of salt.

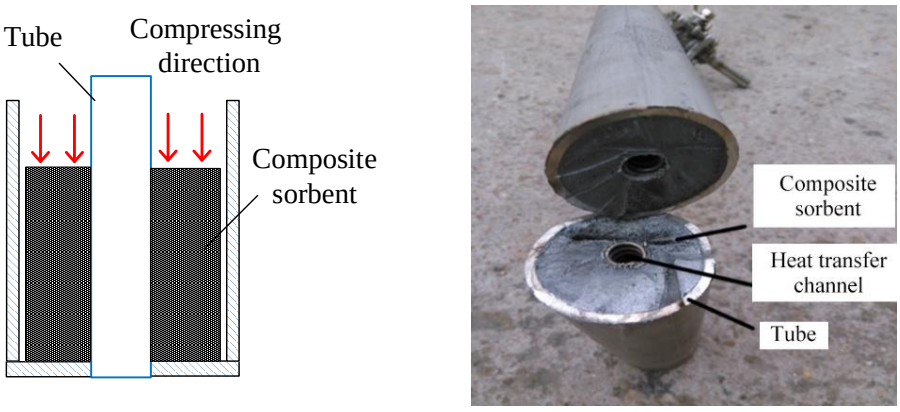

(a) (b)

Fig.10. Schematic diagram of sorption reactor 1 (a) schematic; (b) photo.

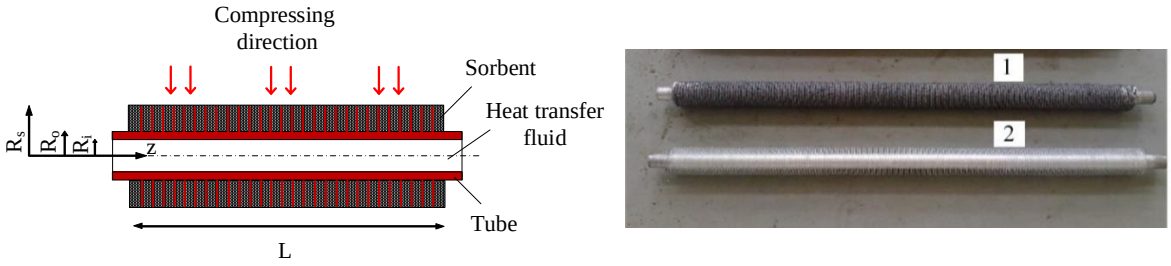

(a) (b)

534 Fig.11. Schematic diagram of sorption reactor 2 (a) schematic; (b) photo: 1-fin tube with sorbent; 2-bare fin tube.

535

536

537

538

539

540

541

542

543

544

545

546

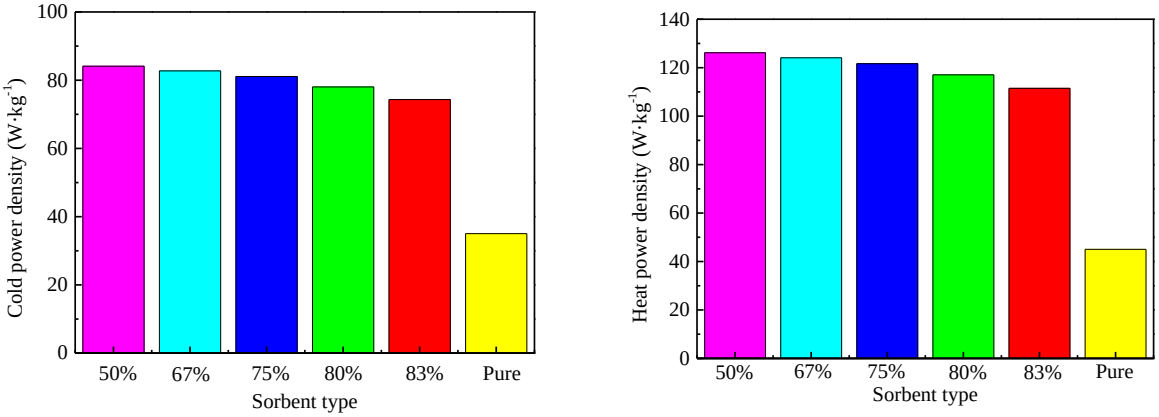

547 Fig.12. Power density of sorption reactor 2 by using the properties of disk sample (a) heat power density; (b)
548 cold power density.

549

550

551

552

553

554

555

556

557

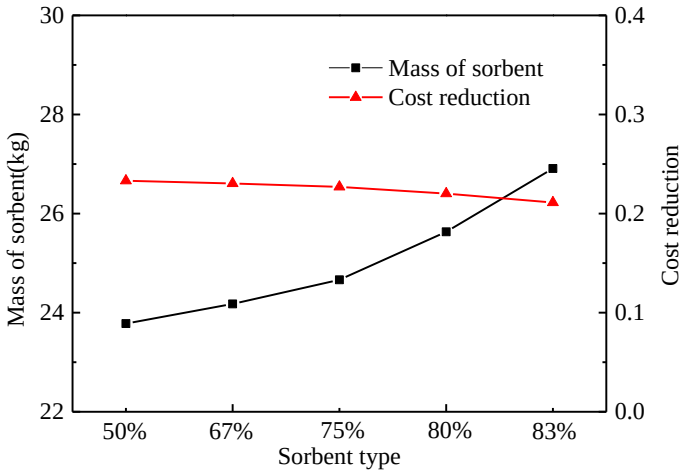

Fig.13. Cost reduction of the novel composite $SrCl_2$ for the system with 2kW required cooling power.

List of Tables

Table 1. Permeability of novel composite $SrCl_2$.

Type of sorbent	Ratio/Density	400	500	600
Disk	50%	4.5×10^{-13}	6.18×10^{-14}	2.46×10^{-14}
	67%	7.2×10^{-13}	1.23×10^{-13}	5.12×10^{-14}
	75%	4.71×10^{-12}	1.65×10^{-12}	2.26×10^{-13}
	80%	7.06×10^{-11}	5.66×10^{-12}	1.12×10^{-12}
	83%	2.91×10^{-10}	8.62×10^{-11}	3.24×10^{-12}
Plate	50%	1.51×10^{-12}	3.05×10^{-13}	9.89×10^{-14}
	67%	2.14×10^{-12}	5.23×10^{-13}	2.01×10^{-13}
	75%	1.51×10^{-11}	5.1×10^{-12}	7.12×10^{-13}
	80%	2.98×10^{-10}	3.16×10^{-11}	4.29×10^{-12}
	83%	9.9×10^{-10}	1.61×10^{-10}	9.14×10^{-12}

613

614 Table 2. The main parameters for sorption reactor 2 in the simulation.

Parameter	Symbol	Value
Metal tube internal radius	R_i	10 mm
Sorbent internal radius	R_o	12 mm
Sorbent external radius	R_s	24 mm
Axial length of the sorbent	L	1000 mm
Flow velocity of heat transfer fluid	u_f	0.16 m·s^{-1}
Porosity of the sorbent	ε	0.3
Cycle maximum temperature	T_{max}	105°C
Cycle minimum temperature	T_{min}	30°C
Evaporating temperature	T_e	5°C
Condensing temperature	T_{con}	30°C
Inlet heat source temperature	$T_{in,\,h}$	110°C
Inlet cooling temperature	$T_{in,c}$	25°C

615

616